Study on β-Chitosan against the binding of SARS-CoV-2S-RBD/ACE2

Gulimiran Alitongbieke[1#] Xiu-min Li[2#] Qi-Ci Wu[1#] Zhi-Chao Lin[2#] Jia-Fu Huang[1] Yu Xue[1] Jing-Na Liu[3] Jin-Mei Lin[4] Tao Pan[5,6] Yi-Xuan Chen[1] Yi Su[1] Guo-Guang Zhang[3] Bo Leng[1] Shu-Wen Liu[3] Yu-Tian Pan[1,3*]

Affiliation

[1] Fujian Engineering Technology Research Center of Fungal Active Substances, 363000, Zhangzhou, China;

[2] Fujian Universities Engineering Technology Research Center of Fungus Industry, 363000, Zhangzhou, China;

[3] School of Biological Science and Biotechnology, Minnan Normal University, 363000, Zhangzhou, China;

[4] College of Chemistry, Chemical Engineering and Environment, Minnan Normal University, 363000, Zhangzhou, China;

[5] Mengdeer (Xiamen) Biotechnology Co., Ltd., 361000, Xiamen, China;

[6] Fujian Maillardkan Biopharmaceutical Co., Ltd., 363000, Zhangzhou, China.

\# These authors contributed equally to this work;

* **Corresponding author**: Prof. Yu-Tian Pan, pyt@mnnu.edu.cn.

ABSTRACT

It has been known that SARS-CoV-2 which is considered similar to SARS-CoV invades human respiratory epithelial cells through interaction with the human angiotensin converting enzyme II (ACE2). In this work, SARS-CoV-2S-RBD and its cell receptor ACE2 were used to investigate the blocking effect and mechanism of β-chitosan to the binding of them. Besides, inhibitory effect of β-chitosan on inflammation induced by SARS-CoV-2S-RBD was also studied. Firstly, Native-PAGE results showed that β-chitosan could bind with ACE2 or SARS-CoV-2S-RBD and the conjugate of β-chitosan and ACE2 could no longer bind with SARS-CoV-2S-RBD. HPLC analyses suggested that was found the conjugate of β-chitosan and SARS-CoV-2S-RBD displayed high binding affinity under the condition of high pressure (40 MPa) compared with that of ACE2 and SARS-CoV-2S-RBD. Furthermore, immunofluorescence detections on Vero E6 cells and hACE2 mice showed that β-chitosan had a significant prevention and treatment effect on SARS-CoV-2S-RBD binding. Meanwhile, SARS-CoV-2S-RBD binding could activate the inflammation signaling pathways of cells and mice, however, β-chitosan could dramatically suppress the inflammations activated by SARS-CoV-2S-RBD. Subsequently, Western blot analyses revealed that the expression levels of ACE2 in experimental groups treated with β-chitosan significantly reduced. However, after the intervention of ADAM17 inhibitor (TAPI), the decreased ACE2 expressions affected by β-chitosan up-regulated correspondingly. The results indicated that β-chitosan has a similar antibody function, which can neutralize SARS-CoV-2S-RBD and effectively block the binding of SARS-CoV-2S-RBD with ACE2. ADAM17 activated by β-chitosan can enhance the cleavage of ACE2 extracellular domain with a catalytic activity of Ang II degradation, and then the extracellular region was released into the extracellular environment. So, β-chitosan could prevent the binding, internalization and degradation of ACE2 with SARS-CoV-2S-RBD and inhibit the activation of inflammatory signaling pathways at the same time. This work provides a valuable reference for the prevention and control of SARS-CoV-2 by β-chitosan.

Keywords: SARS-CoV-2; ACE2; SARS-CoV-2S-RBD; β-chitosan; ADAM17

INTRODUCTION

According to the latest WHO data, novel coronavirus-caused pneumonia (COVID-19) pandemic has spread to more than 200 countries and regions and caused more than 15 million confirmed infections including 600 thousand deaths by now, which has elicited extraordinary responses world-wide. Although SARS-CoV-2 was quickly discovered and identified as the pathogen (Wu, Zhao et al. 2020), so far no successful vaccines or specific drugs could be put into use, the daily numbers of confirmed infections and deaths are still climbing. Therefore, the researches on the pathogenesis of COVID-19 and effective therapeutic goods to prevent and treat the current pandemic have become the most urgent work in the world.

Zhou *et al*. (Zhou, Yang et al. 2020) revealed the finding at a molecular level that 2019-nCoV uses the same cell entry receptor (ACE2) as SARS-CoV basing. Xu *et al.* (Xu, Chen et al. 2020) found that by bioinformatics the Spike protein of SARS-CoV-2 is similar to that of SARS-CoV, suggesting that SARS-CoV-2 can infect host cells by binding to ACE2 on the surface of host cells through Spike protein. Then, Hoffmann *et al.* (Hoffmann, Kleine-Weber et al. 2020) confirmed that on cell level SARS-CoV-2 uses the same receptor ACE2 to enter host cells as SARS-CoV. Soon, the tissues and organs expressing ACE2 aroused much concern. It was reported that ACE2 was not only highly expressed in the lung cells, esophagus upper and stratified epithelial cells but also in absorptive enterocytes from ileum and colon. Thereby, it was inferred that SARS-CoV-2 may bind with ACE2 to invade and damage the relevant tissues of patients (Zhou, Zhou et al. 2004, Fan, Li et al. 2020, Zhang, Kang et al. 2020). Since SARS-CoV-2 and SARS-CoV have similar gene sequence, same binding receptor and similar clinical manifestations, the similar pathogenesis of them may exist. Because of the cell endocytosis induced by the binding of virus and ACE2, ACE2 was almost degraded and Ang II level increased significantly, leading to inflammatory factor storm and multiple organ damage (Oudit, Kassiri et al. 2009). Yan *et al.* (Yan, Zhang et al. 2020) firstly presented cryo-electron microscopy structures of full-length human ACE2 and pointed out that spike protein of SARS-CoV-2 (SARS-CoV-2-RBS) binds to the extracellular peptidase domain of ACE2 mainly through polar residues. Wrapp *et al.* (Wrapp, Wang et al. 2020) determined a 3.5-angstrom-resolution structure of the 2019-nCoV Spike protein by cryo-electron microscopy, and demonstrated that the affinity of ACE2 binding to 2019-nCoV Spike was 10~20 folds higher than that to SARS-CoV

Spike, further revealing the higher infectivity and pathogenicity rate of 2019-nCoV than SARS-CoV. Thus, it is of great significance to explore the blocker for the binding of SARS-CoV-2 and ACE2 as soon as possible for the prevention and control of COVID-19.

ACE2 which can protect from severe acute lung failure is selected as the receptor of SARS-CoV-2, which posed a dilemma for the targeted treatment of ACE2. Many reports have confirmed that the genes of ACE2 and ACE originated from the same ancestor (Huang, Sexton et al. 2003, Towler, Staker et al. 2004) , so ACE2 is closely related to ACE in human body. It was reported that chitosan binds to the active site of ACE to inhibit the activity to achieve the antihypertensive effect (Huang, Mendis et al. 2005, Jo, Ha et al. 2013). Since no toxic and side effects on human body, chitosan has become one of the research hotspots of antihypertensive functional food and adjuvant drugs. According to the structure comparisons of ACE and ACE2 (PDB ID codes 1o8a and 1r42, respectively), both of them have the same active site with an amino acid sequence (HEMGH) for zinc ion combination area. It implies that ACE2 can bind with chitosan because of the same active site with ACE. If the combination can prevent SARS-CoV-2 binding with ACE2 and maintain the antihypertensive activity of ACE2, this work will have great scientific significance. At present, there is no report about chitosan binding ACE2 to inhibit SARS-CoV-2 infection.

Chitosan is a partially deacetylated derivative of chitin. Owing to its unique properties such as biodegradability, biocompatability, biological activity, and capacity of forming polyelectrolyte complex with anionic polyelectrolytes, chitosan has been widely applied in the food and cosmetics industry as well as the biomedical field in relation to tissue engineering, and the pharmaceutical industry relating to drug delivery. Chitosan occurs in three distinct crystalline polymorphic forms: α-, β-and γ-chitosan (Meyer and Mark 1928, Meyer and Pankow 1935, Rudall 1963). Chitosan is normally dissolved in acidic conditions and precipitated when pH is above 7, which greatly limited its applications in cells and animals under the physiological environment. Compared with α-chitosan, β-chitosan has weaker intramolecular and intermolecular hydrogen bonding forces, higher solubility and biological activity. In this work, in order to provide a new strategy for the prevention and control SARS-CoV-2S, β-chitosan (**Mendel®**), which could be stably dissolved in a buffer solution system with similar pH (7.4) in normal human body fluid, was utilized to investigate the blocking effect and mechanism of SARS-CoV-2S/ACE2 binding.

RESULTS

I Molecular interaction model *in vitro* of β-chitosan against the binding of SARS-CoV-2S-RBD with ACE2

The co-incubation mixture collected were analyzed by Native-PAGE. As shown in **Figure 1B**, the grey values of ACE2 and SARS-CoV-2S-RBD incubated with β-chitosan (lane 3 and 5) fell 95.8% and 94.8% compared with those of ACE2 and SARS-CoV-2S-RBD (lane 2 and 4), respectively. It indicated that β-chitosan showed a strong binding affinity to ACE2 and SARS-CoV-2S-RBD under normal physiological condition *in vitro*. In addition, after the binding of ACE2 with SARS-CoV-2S-RBD, the grey value in lane 7 significantly reduced compared with that of ACE2 or SARS-CoV-2S-RBD, respectively, indicating that ACE2 is strongly bound to SARS-CoV-2S-RBD. With the addition of β-chitosan, the grey value in lane 7 decreased significantly, which demonstrated that β-chitosan has an obvious effect on the conjugate of SARS-CoV-2S-RBD and ACE2.

Figure 1

Can the conjugate of β-chitosan and ACE2 (named as β-chitosan~ACE2) bind with SARS-CoV-2S-RBD again? To answer this question, the experiment was designed to further verify that as shown in **Figure 1A**. Under the condition of excessive ACE2 relative to β-chitosan, the same amount of ACE2 were mixed and incubated with different gradient amounts of β-chitosan. Then, the same excessive amount of SARS-CoV-2S-RBD were added for co-incubation again. Finally, the binding interaction was judged by Native-PAGE. With the increase of β-chitosan, β-chitosan~ACE2 would correspondingly increase and surplus ACE2 would present a decrease trend. As a specific receptor binding domain of ACE2, the additional SARS-CoV-2S-RBD would prefer to bind with the surplus ACE2. When the equal amounts of SARS-CoV-2S-RBD were added to bind with the surplus ACE2, whether the final surplus SARS-CoV-2S-RBD could bind with ~ACE2 and/or ~β-chitosan in the conjugate? Hereafter, the remaining SARS-CoV-2S-RBD might suffer from the following three situations (**Figure 1A**): (1) When only ~β-chitosan or ~ACE2 could continually bind with the surplus SARS-CoV-2S-RBD, then eventually the remaining SARS-CoV-2S-RBDs would be the same and grey values would show no difference; (2) When both ~β-chitosan and ~ACE2 could continually bind with surplus SARS-CoV-2S-RBD, then the surplus SARS-CoV-2S-RBD and grey values would gradually decrease; (3) When

neither ~β-chitosan nor ~ACE2 could continually bind with the surplus SARS-CoV-2S-RBD, finally the surplus of SARS-CoV-2S-RBD and grey values should gradually increase. Finally, Native-PAGE results showed that grey values of SARS-CoV-2S-RBD increased gradually (lane 8~10 in **Figure 1B**), which is in accordance with the third speculation. It indicated that β-chitosan can bind with ACE2 and block the binding of SARS-CoV-2S-RBD with ACE2, which shows an effect of preventing virus infection.

HPLC were also used to analyze the co-incubation mixture collected. As shown in **Figure 1D**, for ACE2 there was only a characteristic peak in 9.17 min (**Figure 1D-1**), and two characteristic peaks were found for SARS-CoV-2S-RBD with the retention times (t_R) of 10.081 min and 11.765 min (**Figure 1D-2**), respectively. It was speculated that SARS-CoV-2S-RBD composed of polymers and monomers. Moreover, there was no characteristic peak for β-chitosan in the current detection system (**Figure 1D-3**). After co-incubation at 37 °C for 20min, two characteristic peaks for the conjugate of SARS-CoV-2S-RBD and ACE2 were found (**Figure 1D-4**). Compared with ACE2 and SARS-CoV-2S-RBD, t_Rs shifted to 8.187min and 9.086min, respectively. It indicated that the combination between ACE2 and SARS-CoV-2S-RBD might be followed by the change of t_R. There was only one peak (9.17 min) for the co-incubation mixture of β-chitosan and ACE2 with a similar peak area to ACE2 as shown in **Figure 1D-1**. It suggested that the conjugate of β-chitosan and ACE2 in atmospheric pressure dissociated under the condition of high pressure (40 MPa), which indicated the binding affinity of β-chitosan and ACE2 is relative weak. Interestingly, the conjugate of β-chitosan and SARS-CoV-2S-RBD showed only one characteristic peak in 10.81 min with a similar peak area to SARS-CoV-2S-RBD in **Figure 1D-2** and the second peak disappeared (**Figure 1D-6**). It illustrated that the binding affinity of β-chitosan and SARS-CoV-2S-RBD is very strong. Similar experiment was carried out to verify whether the conjugate of β-chitosan and SARS-CoV-2S-RBD can bind with ACE2. As shown in **Figure 1D-7**, only one characteristic peak of ACE2 was found in the mixture and the peak area was similar to ACE2 (**Figure 1D-1**). It revealed that the conjugate of β-chitosan and SARS-CoV-2S-RBD could not bind with ACE2, which was consistent with of Native-PAGE analysis. If β-chitosan~ACE2 dissociated at 40 MPa, the dissociative ACE2 would prior to bind with SARS-CoV-2S-RBD, leading to similar results to that in **Figure 1D-4**. However, the results showed great significant difference, indicating that β-chitosan might interfere in the binding of ACE2 and SARS-CoV-2S-RBD.

Therefore, results of *in vitro* molecular model shows that β-chitosan possesses a significant neutralization of SARS-CoV-2S-RBD, thereby blocking the binding of SARS-CoV-2S-RBD and ACE2, suggesting that β-chitosan can protect ACE2 from SARS-CoV-2S-RBD binding.

II Vero E6 Cell model *in vitro* of β-chitosan against the binding of SARS-CoV-2S-RBD with ACE2

The results of cell immunofluorescence assay showed (**Figure 2A**) that ACE2 (red) and SARS-CoV-2S-RBD (green) presented strong fluorescence intensities after the addition of SARS-CoV-2S-RBD into Vero E6 cells. Moreover, the significant co-location of ACE2 and SARS-CoV-2S-RBD was found, implying that SARS-CoV-2S-RBD can firmly bind to ACE2. After β-chitosan and SARS-CoV-2S-RBD added successively, the fluorescence intensities of ACE2 and SARS-CoV-2S-RBD significantly reduced. It suggested that β-chitosan could down-regulate the ACE2 expression in Vero E6 cells, resulting in the lower binding probability of SARS-CoV-2S-RBD with Vero E6 cells. As shown in **Figure 2A**, when SARS-CoV-2S-RBD preceded β-chitosan into Vero E6 cells, the co-location of ACE2 and SARS-CoV-2S-RBD relatively reduced, indicating that β-chitosan can intervene in the binding of SARS-CoV-2S-RBD with Vero E6 cells. When the excessive β-chitosan was mixed with SARS-CoV-2S-RBD and then the mixtures were added into Vero E6 cells, the fluorescence intensities of ACE2 and SARS-CoV-2S-RBD significantly decreased and no co-location was found, revealing that β-chitosan has a special neutralizing activity against SARS-CoV-2S-RBD. In addition, it was also observed that the additional β-chitosan alone significantly lowered the ACE2 expression in Vero E6 cells.

Figure 2

Flow Cytometry (FCM) was used to detect the intervention effect of β-chitosan on Vero E6 cells infected by SARS-CoV-2S-RBD (**Figure 2B**). Under the same parameter, 8000 cells were selected for analysis, and the co-location of each experimental group was compared. It was found that the co-location of ACE2 and SARS-CoV-2S-RBD reached 33.6% (green line in **Figure 2B**) after 10 min treatment of SARS-CoV-2S-RBD in Vero E6 cells. Then, β-chitosan was added into the above system 10 min later and the co-location proportion fell to 22.4% (yellow line in **Figure 2B**), which exhibits that the additional β-chitosan could decrease the binding rate of SARS-CoV-2S-RBD to Vero E6 cells. When both β-chitosan and SARS-CoV-2S-RBD were added successively

in Vero E6 cells for 10 min (red line in **Figure 2B**), respectively, the co-location proportion was only 11.4%, indicating that β-chitosan could significantly block the binding of SARS-CoV-2S-RBD with Vero E6 cells. When the excessive β-chitosan was mixed with SARS-CoV-2S-RBD and then the mixtures were added into Vero E6 cells, the co-location proportion was only 6.91%, which further proves that β-chitosan has a neutralizing activity against SARS-CoV-2S-RBD.

Western blot was used to detect the relative proteins in the inflammation signaling pathway. p-JNK, p-IKK, p-IκB and p-c-jun are known representative of inflammation-related proteins. Nur77, an orphan member of the nuclear receptor superfamily, is expressed in macrophages following inflammatory stimuli (Hu, Luo et al. 2017). It was found that the expressions of Nur77, p-JNK, p-IKK, p-IκB and p-c-jun significantly up-regulated after SARS-CoV-2S-RBD intervention in Vero E6 cells for 10 min (**Figure 2C**). However, those expressions obviously down-regulated when β-chitosan was added to treat for 10 min in Vero E6 cells affected by SARS-CoV-2S-RBD. The results indicated that SARS-CoV-2S-RBD could induce the inflammation in cells. The additional β-chitosan could obviously inhibit the activation of inflammation signaling pathways, presenting an anti-inflammatory effect.

III Animal model *in vivo* of β-chitosan against the binding of SARS-CoV-2S-RBD with ACE2

FITC tag is often used to observe β-chitosan metabolism *in vivo*. However, the dissociation of β-chitosan-FITC in the metabolic process can lead to the authenticity deviation of β-chitosan distribution. Thus, β-chitosan was directly given intranasally and then calcofluor white (CFW) was used to observe the metabolic distribution (Bhavasar, Goje et al. 2010). After intranasal administration, the metabolism and distribution of β-chitosan in the lung tissue of mice was observed in 1 hour, 2 hour and 4 hour, respectively. It was found that the blue fluorescent of β-chitosan dyed with CFW was clearly distributed in the lung tissue of mice (**Figure 3A**). The above results indicated that by intranasal administration β-chitosan can spread and attach to those cells of lung tissue in a certain time, which provides a prerequisite for the further evaluation of the antiviral infection ability of β-chitosan in the lung tissue.

Figure 3

The prevention and treatment effect of morphological lesion induced by SARS-CoV-2S-RBD in the lung tissue of mice was further observed (**Figure 3B**). It was found

that the lung organ of hACE2 mice infected with SARS-CoV-2S-RBD obvious swelled. However, the lung organ of the prevention and treatment groups treated with β-chitosan showed no difference from the normal control group, revealing that β-chitosan could inhibit the pathological changes of the lung organ of hACE2 mice caused by SARS-CoV-2S-RBD. Moreover, it was also observed that SARS-CoV-2S-RBD did not cause lung organ enlargement in wild type (WT) mice, which indicated that SARS-CoV-2S -RBD has a specific effect to hACE2 on morphological lesion.

ACE2 expression and its co-localization with SARS-CoV-2S-RBD for WT and hACE2 mice were detected by immunofluorescence. The two types of mice presented a little difference in cell numbers and the fluorescence intensities of ACE2 and SARS-CoV-2S-RBD. For WT mice, the number of cells per unit area and the fluorescence intensity of ACE2 increased significantly in SARS-CoV-2S-RBD infected group as shown in **Figure 3C**. However, the cells for hACE2 mice obvious decreased and no obvious immunofluorescence of ACE2 was discovered in SARS-CoV-2S-RBD infected group. Moreover, similar phenomenons were found for the two types of mice. It was found that a visible immunofluorescence of SARS-CoV-2S-RBD and the co-localization of SARS-CoV-2S-RBD and ACE2, implying that the lung tissue cells of WT and hACE2 mice can also bind to SARS-CoV-2S-RBD through their ACE2 receptor. For the prevention groups (treated with β-chitosan and SARS-CoV-2S-RBD successively) and treatment groups (treated with SARS-CoV-2S-RBD and β-chitosan successively), no obvious immunofluorescence of SARS-CoV-2S-RBD was found, which indicated that β-chitosan can block the binding of SARS-CoV-2S-RBD with the lung tissue cells of the two types of mice and present a therapeutical effect.

The expressions of ACE2 and inflammation-related proteins were analyzed and compared by Western Blot. For the groups infected with SARS-CoV-2S-RBD (SARS-CoV-2S-RBD group), ACE2 expression distinctly reduced in comparison with the control group for WT and hACE2 mice. For the prevention groups and treatment groups, ACE2 expressions of the two types of mice obviously decreased compared with those of SARS-CoV-2S-RBD groups (**Figure 3D**). In addition, for the expression levels of inflammation-related proteins (such as p-JNK and p-c-jun), SARS-CoV-2S-RBD groups displayed obviously up-regulated expression levels compared with the control group (**Figure 3D**). However, the expression levels of the experimental groups intervened with β-chitosan clearly down-regulated. The results indicated that β-chitosan could affect the hACE2 expression to decrease SARS-CoV-2S-RBD infection.

SARS-CoV-2S-RBD intervention can promote inflammation in the lung tissue, however, β-chitosan can obviously inhibit the activation of inflammation-related signaling pathways and present an anti-inflammatory effect. The above results of animal model are basically consistent with those of cell model.

IV Regulation of ACE2 expression by β-Chitosan

The above results found that β-chitosan could significantly down-regulate the ACE2 expressions in Vero E6 cells and lung tissue cells of hACE2 mice. However, the down-regulated ACE2 expressions did not cause, on the contrary, β-chitosan could inhibit the inflammation signal activated by SARS-CoV-2S-RBD and has no influence on the antihypertensive effect. Those indicate that the down-regulated expression of ACE2 affected by β-chitosan has no influence on the antihypertensive and anti-inflammatory effect, which implies that there might be another reason for the down-regulated expression of ACE2. Kuba reported that ACE2 could be cut by ADAM17 metalloproteinase which hindered the binding of SARS and ACE2 (Kuba, Imai et al. 2010). However, whether the down-regulated expression of ACE2 is related to ADAM17 activity? Thus, ADAM17 inhibitor was used to verify that issue through immunofluorescence method and Western Blot.

Results showed that β-chitosan could significantly down-regulate the ACE2 expressions in Vero E6 cells. When the ADAM17 inhibitor (TAPI) was added in advance, ACE2 expression up-regulated significantly compared with that of no TAPI group. That indicated that the decreased ACE2 expression regulated by β-chitosan is caused through the activation of ADAM17. Moreover, the active ADAM17 could improve the cleavage of ACE2 extracellular juxtamembrane region with a catalytic activity of Ang II degradation. Then the catalytically active ectodomain was released into the extracellular environment, leading to the decreased binding of cell and SARS-CoV-2S-RBD, which presented an illusion of down-regulated ACE2 expression. Moreover, the shedding extracellular part of ACE2 still has the catalytic activity to degrade Ang II, displaying an antihypertensive function.

Figure 4

DISCUSIONS

In this work, the binding of SARS-CoV-2S-RBD and β-chitosan was found by Native-PAGE and HPLC. Interestingly, β-chitosan can firmly bind with SARS-CoV-

2S-RBD without dissociation under high pressure. Thus, a special *in vitro* experiment at a molecular level was designed to testify that the conjugate of β-chitosan and ACE2 could no longer bind with SARS-CoV-2S-RBD. Cell immunofluorescence results displayed that SARS-CoV-2S-RBD interacted with β-chitosan extracellularly could not bind with ACE2 in Vero E6 cells. Thus, β-chitosan plays an important role as antibody in neutralizing SARS-CoV-2S-RBD and effectively blocking the binding of SARS-CoV-2S-RBD with ACE2, finally preventing the viral infection risk.

In the human body, ACE is a kind of angiotensin converting enzyme which can catalyze angiotensin I (Ang I) to angiotensin II (Ang II). Ang II plays a crucial role in contracting blood vessels and promoting inflammation through angiotensin type 1 receptor (AT1R). However, ACE2 plays a different role that can catalyze Ang II to vasodilator Ang 1~7 which can dilate blood vessels and inhibit inflammation through Mas receptor. Thus, there may exist a system formed with the axes of ACE-Ang II-AT1R and ACE2-Ang 1~7-Mas to maintain the balance of blood pressure in the human body (Clarke and Turner 2012, Jiang, Yang et al. 2014). Because of the cell endocytosis induced by the binding of SARS-CoV-2 and ACE2, ACE2 was almost consumed and Ang II level increased obviously, leading to inflammatory factor storm and multiple organ damage (Oudit, Kassiri et al. 2009, Huang, Wang et al. 2020). Therefore, once infected by SARS-CoV-2 whether ACE2 is an enemy or a friend to human beings has become a hotly debated scientific issue. Acute respiratory distress syndrome (ARDS) is one of the leading reasons of death for patients infected with COVID-19 and SARS. The relationship between ARDS and ACE2 has attracted much attention. The finding from Imai group (Imai, Kuba et al. 2005) showed that ARDS lesions in mice with ACE2 gene knockout were significantly more severe than those in the control group, while the application of recombinant ACE2 could significantly reduce the occurrence of ARDS in mice, suggesting that ACE2 expression has an obvious protective effect on ARDS in mice. Kuba *et al*. (Kuba, Imai et al. 2005) reported that the expression of ACE2 was down-regulated *in vivo* and *in vitro* by recombinant SARS-CoV-S protein, resulting in pulmonary edema, lung function deterioration and ARDS in mice. It has been reported by Oudit that ACE2 expression in myocardium in mice and patients infected with

SARS-CoV decreased significantly (Oudit, Kassiri et al. 2009). These results suggest that ACE2 expression level is closely related to the severity of SARS lesions. Currently, the expression levels of ACE2 in cardiopulmonary tissues of COVID-19 patients has not been reported. Liu *et al* (Liu, Yang et al. 2020) found that Ang II levels in COVID-19 patients plasma were significantly higher than that of healthy controls, moreover, Ang II level was linearly related to virus titer and lung injury degree, indirectly testifying that those phenomenons were induced by the drop of ACE2 expression level.

Native-PAGE results suggested that ACE2 can be bound with β-chitosan to block SARS-CoV-2S-RBD binding again. Immunofluorescence and FCM results based on cell and animal model found that β-chitosan has a significant prevention and treatment effect on SARS-CoV-2. Western Blot test showed that the expression levels of ACE2 in Vero E6 cells and hACE2 mice infected with SARS-CoV-2S-RBD were significantly decreased and inflammations were also activated. Compared to the individual SARS-CoV-2S-RBD group, ACE2 expression levels in each group of cells or tissues treated with β-chitosan obviously decreased. However, the decreased ACE2 induced a significant inhibitory effect on inflammation caused by SARS-CoV-2S-RBD instead of inflammation. This is an interesting and important discovery. For the known regulation mechanisms of ACE2 expression, ACE2 expression down-regulated because of the binding, internalization and degradation of ACE2 with virus. Moreover, transmembrane protease ADAM17 can cleave the juxtamembrane region of ACE2 and then release the active extracellular domain which can catalyze the degradation of Ang II into the extracellular environment (Kuba, Imai et al. 2010, Patel, Clarke et al. 2014). Thus, it is speculated whether there was a certain interaction mechanism against SARS-CoV-2 harm among β-chitosan, ADAM17 and ACE2. Accordingly, ADAM17 inhibitor (TAPI) was used to testify the speculation and the result showed that the decreased ACE2 expression levels in experimental groups induced by β-chitosan were suppressed by ADAM17 inhibitor. Compared with no inhibitor group, ACE2 expression level significantly raised (* $P < 0.05$; * * $P < 0.01$). It suggested that β-chitosan can activate ADAM17 to enhance the cleavage of the extracellular juxtamembrane region of ACE2, and then release the extracellular domain with catalytic activity into the extracellular environment, reducing the binding and internalization of SARS-CoV-2S-RBD with susceptible cells. Moreover, the shedding extracellular region of ACE2 can still maintain the catalytic activity to degrade Ang II and inhibit inflammations. In summary,

the mechanism of β-chitosan against SARS-CoV-2 by blocking SARS-CoV-2S-RBD/ACE2 binding can be summarized in **Figure 5**. Therefore, ADAM17 is a most probably noteworthy target for the treatment of SARS-COV-2.

Figure 5

Recently, Waradon Sungnak's reported (Sungnak, Huang et al. 2020) that ACE2 and TMPRSS2 were highly expressed in nasal goblet cells and ciliated cells which could produce mucus. Moreover, the virus concentration in nasal swabs from respiratory disease patient caused by SARS-CoV-2 was higher than that of pharyngeal swabs, suggesting that nasal passage may be a channel for initial infection and transmission of virus. By intranasal administration, we found that β-chitosan can be effectively distributed in lung tissue in the test time. This result provides a necessary condition for β-chitosan to block the binding of SARS-CoV-2S-RBD with ACE2 *in vivo*. Furthermore, β-chitosan, which can be safely degraded, has a good biocompatibility in brain tissue of rats (Zhou, Zhou et al. 2004). Kean also found that β-chitosan shows no toxicity by acute toxicity test on mice and no irritation to eyes and skin of rabbit (Kean and Thanou 2010). Thus, β-chitosan by intravenous injection is safe to human body. In this paper, the infection effect of SARS-CoV-2 and the prevention and therapeutic effect of β-chitosan were compared between WT and hACE2 mice. The results suggested that SARS-CoV-2S-RBD could induce severe inflammation in the whole lung of hACE2 mice, but no similar pathological phenomenon was found in WT mice, which was basically in accordance with the results of Bao *et al*'s work (Bao, Deng et al. 2020). However, immunofluorescence in tissues displayed that lung tissue cells of WT and hACE2 mice could bind with SARS-CoV-2S-RBD. The results indicated that SARS-CoV-2S-RBD has different pathogenic effects on WT mice and hACE2 mice, especially high pathogenicity to hACE2 host, suggested that hACE2 animal model is an indispensable scientific tool for anti-SARS-CoV-2S drug screening to human beings.

In this work, the effect and mechanism of β-chitosan against the binding of SARS-CoV-2S-RBD/ACE2 were investigated based on three levels (molecular, cellular and animal). Results revealed that β-chitosan has a significant prevention and treatment effect of SARS-CoV-2 by blocking the binding of SARS-CoV-2S-RBD/ACE2 and

inhibiting the inflammations. It is a promising and important research with a great value and application prospect for anti-SARS-CoV-2S by β-chitosan. With the current epidemic raging, it is time to share our research results in a timely manner and carry on with the burden of further research.

Materials and methods

Ethics statement

All procedures in this study involving animals were reviewed and approved by Minnan Normal University Animal Ethics and Welfare Committee (MNNU-AEWC-2020001).

Antibody and reagents

Anti-His-Tag, Anti-p-IKK, Anti-p-JNK, Anti-p-c-jun were purchased from Affinity Biosciences, Inc. (Cincinnati, OH, USA). Anti-ACE2 was purchased from Abcam (Cambridge, UK). Anti-β-actin was purchased from Cell Signal Technology (Beverly, MA, USA). HRP-conjugated anti-mouse IgG and HRP-conjugated anti-rabbit IgG were purchased from Abcam (Cambridge, UK). Calcofluor white (CFW) was purchased Shanghai yuanye Bio-Technology Co., Ltd. (Shanghai, China). TAPI-1 was purchased from APExBIO Technology LLC (Houston, USA). SARS-CoV-2S-RBD and ACE2 protein were purchased from Novoprotein Scientific Inc. (Shanghai, China). FITC-conjugated sheep and donkey anti-mouse IgG, cy3-conjugated sheep and donkey anti-rabbit IgG and His-Tag antibody were purchased from Affinity Biosciences, Inc. (Cincinnati, USA).

Dulbecco's modified Eagle's medium (DMEM) were bought from Invitrogen Corp. (Carlsbad, USA). 10% fetal bovine serum (10%FBS) was purchased from Thermo Fisher Scientific Co., Ltd. (Waltham, USA). β-Chitosan was obtained from Mengdeer (Xiamen) Biotechnology Co., Ltd. (Xiamen, China). Other chemicals and reagents used in this study were analytical reagent grade and used as received.

Cell lines

Vero E6 cells were maintained in Dulbecco's Modified Eagle Medium containing 10% fetal bovine serum and a humidified atmosphere with 5% CO2 at 37ºC.

Mice

Groups of 8-week-old hACE2 and wild-type male mice (C57BL/6 background) were purchased from the GemPharmatech (Nanjing, China). All of the mice were

maintained in animal room with 12-hours light/12-hours dark cycles at Laboratory Animal Center in Min Nan Normal University (China).

Binding of β-chitosan with ACE2 or SARS-CoV-2S-RBD

Proteins (SARS-CoV-2S-RBD and ACE2) and β-chitosan were dissolved in 0.02 M Tris-HCl buffer solution (pH 6.8) in advance. According to the relative molecular weights of SARS-CoV-2S-RBD and ACE2, and the detection limit of Native PAGE, SARS-CoV-2S-RBD was firstly mixed with different amount of β-chitosan and incubated under 37 °C for 20 mins. Then, ACE2 was added into the co-incubation mixture for another incubation in the same way. The mixture samples collected were analyzed by Native-PAGE and SEC-HPLC.

Cell experiments

Vero-E6 cells were cultured in Dulbecco's modified Eagle's medium (DMEM, Invitrogen, Carlsbad, USA) supplemented with 10% fetal bovine serum (FBS), 50 units/mL penicillin, and 50 μg/mL streptomycin in a humidified atmosphere (5% CO_2) at 37°C. When the cells grow to 80%, they were treated according to experiment design.

At the beginning of the experiment, 8 μM TAPI-1 was added to Vero-E6 cells 30 minutes in advance.

Animal experiments

For the animal experiments, specific pathogen-free, male transgenic hACE2 mice were obtained from the experimental animal center of GemPharmatech (Nanjing, China). Transgenic mice were generated by microinjection of the mouse *ACE2* promoter which can drive human *ACE2* coding sequence into the pronuclei of fertilized ova from ICR mice, and then human ACE2 integrated was identified by PCR as previous report (Yang, Deng et al. 2007). The human ACE2 mainly expressed in lung, heart, kidneys and intestines of transgenic mice. The dosage of β-chitosan was intranasally administrated according to the method published previously (Zheng, Qu et al. 2016). SARS-CoV-2S-RBD and β-chitosan were inoculated intranasally into hACE2 and WT mice at a dosage of 10 mg/kg body weight, respectively, and an equal volume of PBS was used as control. Mice were dissected to collect different tissues to observe the histopathological changes.

Flow Cytometry

When Vero-E6 cells grow to 80%, they were treated according to the experimental design. Cells obtained from the culture were washed with PBS once. Then, the cells were properly digested with trypsin and then centrifuged. Subsequently, the cells was

washed with PBS twice and fixed overnight at 4°C with 200 μL precooled paraformaldehyde (4%). Fixed cells were collected after centrifugation and washed twice with precooled PBS, sealed with 10% sheep serum for 15 min, washed twice with precooled PBS. Then, His-Tag antibody (1:200, Affinity, T0009, USA) and ACE2 antibody (1:100, Abcam, ab15348, USA) were added for overnight at 4°C; Subsequently, cells were washed twice with PBS. With the addition of three secondary antibodies FITC-conjugated sheep anti-mouse IgG (1:300, Affinity, USA), Cy3-conjugated sheep anti-rabbit IgG (1:300, Affinity, USA) and DAPI (1:300, Affinity, USA)), cells were re-suspended and incubated in dark at 37 °C for 60 min. After staining, the cells were washed, re-suspended in precooled PBS and detected with flow cytometry (Flowsight, Merk Millipore, USA). Instrument was adjusted according to the reported procedure (Terrazas, Oghumu et al. 2015). About 8000 cells were acquired to be detect. Co-localization of S-RBD-His-FITC and ACE2-cy3 was analyzed using co-localization analysis application Wizard in IDEAS software.

CFW

Paraffin sections were dewaxed to water, washed with distilled water and dried. CFW fluorescent staining solution was added to dye the sections in dark for 10 min. Then, the sections was washed it in distilled water and performed routine HE staining after the discard of the dye solution. Distilled water slightly washed, gradient ethanol dehydration, xylene transparent, neutral gum sealing.

Confocal Microscopy

For immunofluorescence on cell culture, cells mounted on glass slides were permeabilized with PBS containing 0.1% TritonX-100 and 0.1mol/L of glycine for 15min, and blocked with 1% donkey serum albumin in PBS for 30min at room temperature, followed by an incubation with primary antibodies (His-Tag (1:200, affinity, T0009) and ACE2 (1:200, Abcam,ab15348)) in PBS for overnight at 4°C and detected by FITC-labeled anti-donkey IgG(1:400) or anti-donkey IgG conjugated with Cy3(1:400) at room temperature for 1h. Cells were costained with 4', 6-diamidino-2-phenylindole (DAPI) to visualize nuclei. The images were taken under a fluorescent microscope (CarlZeiss) or a confocal lasers canning microscope system (Leica DMi8).

For section immunofluorescence, fresh samples were isolated and fixed in 4% paraformaldehyde solution at 4°C overnight. After dehydration through gradient

ethanol, samples were embedded in paraffin and sectioned. 4 µM paraffin sections were deparaffifinised in xylene and rehydrated in a series of graded alcohols. Antigen retrievals were performed in citrate buffer (pH6) with a microwave for 30 min at 95 ºC followed by a 30-min cool-down period at room temperature. Briefly, endogenous peroxidase was quenched in 3% H_2O_2 for 20 min, followed by blocking reagent for 1 hour at room temperature. Primary antibody was incubated for overnight in a humidified chamber at 4°C, followed by detection using the by FITC-labeled anti-donkey IgG (1:400) or anti-donkey IgG conjugated with Cy3 (1:400) at room temperature for 1h. In a serial fashion, each antigen was labeled by distinct fluorophores. Multiplex antibody panels applied in this study are: His-Tag (1:200, affinity, T0009) and ACE2 (1:200, Abcam, ab15348); after all the antibodies were detected sequentially, the slices were imaged using the confocal laser scanning microscopy platform Leica.

Native-PAGE Analysis

6% resolving gel and 5% condensing gel were used in the Native-PAGE analysis. The protein solution was diluted to the concentration of 0.5~2.0 mg/mL. The amount of loading sample was 2µL of protein marker and 20µL of protein sample. The protein migration was performed under 100 V for 120 min. The gel was visualized with silver staining after electrophoresis according to the method published previously (Nesterenko, Tilley et al. 1994) with some modifications. The stained protein gel was scanned using the Gel Doc 2000 imaging system (Bio-Rad, Hercules, CA, USA) and analyzed by Quantity One software (Bio-Rad, Hercules, CA, USA).

SEC-HPLC Analysis

The analytical SEC-HPLC was performed with Agilent 1200 HPLC system (Agilent Technologies, Santa Clara, CA, USA) using the Waters Ultrahydrogel™ 1000 column (12 µm, 7.8 mm × 300 mm, Waters, USA). The mobile phase of 0.2 M Tris-HCl buffer (pH 6.8) was used after 0.22 µm membrane filtration and degassing. The operation flow rate was 1 mL/min, and the sample injection volume was 20 µL. The chromatographic run was monitored on-line at 280 nm by an UV detector. The integrated peak areas of each component were used to evaluate protein amount.

Western blot

Cell and mice tissues were homogenized in cell lysis buffer. Proteins from cell or tissue lysates were separated with SDS-PAGE gel and transferred to nitrocellulose membrane. The membrane was blocked in 5% non-fat milk for 1 h at room temperature, incubated with primary antibodies (including anti-ACE2, anti-p-IKK, anti-p-JNK, anti-

p-c-jun, β-actin) overnight at 4°C. Then the membrane was washed by TBST for 3 times and incubated with secondary antibody (HRP-linked anti-immunoglobulin) for 1h. The final immunoreactive products were observed by Omega Lum C Gel Imaging system (Aplegen, USA).

Statistical analysis

All data were analyzed with GraphPad Prism 8.0 software. Two-tailed Student's *t*-tests were applied for statistical analysis. For all graphs, a two-sided *P* value < 0.05 was considered statistically significant (*$P < 0.05$, **$P < 0.01$).

Acknowledgement

REFERENCES

Bao, L., W. Deng, B. Huang, H. Gao, J. Liu, L. Ren, Q. Wei, P. Yu, Y. Xu, F. Qi, Y. Qu, F. Li, Q. Lv, W. Wang, J. Xue, S. Gong, M. Liu, G. Wang, S. Wang, Z. Song, L. Zhao, P. Liu, L. Zhao, F. Ye, H. Wang, W. Zhou, N. Zhu, W. Zhen, H. Yu, X. Zhang, L. Guo, L. Chen, C. Wang, Y. Wang, X. Wang, Y. Xiao, Q. Sun, H. Liu, F. Zhu, C. Ma, L. Yan, M. Yang, J. Han, W. Xu, W. Tan, X. Peng, Q. Jin, G. Wu and C. Qin (2020). "The pathogenicity of SARS-CoV-2 in hACE2 transgenic mice." Nature.

Bhavasar, R. S. K., S. K. Goje, A. A. Takalkar, S. M. Ganvir, V. K. Hazarey and S. R. Gosavi (2010). "Detection of Candida by Calcofluor White." Acta Cytologica **54**(5): 679-684.

Clarke, N. E. and A. J. Turner (2012). "Angiotensin-converting enzyme 2: the first decade." International Journal of Hypertension **2012**: 307315.

Fan, C., K. Li, Y. Ding, W. L. Lu and J. Wang (2020). "ACE2 Expression in Kidney and Testis May Cause Kidney and Testis Damage After 2019-nCoV Infection." medRxiv: 2020.2002.2012.20022418.

Hoffmann, M., H. Kleine-Weber, N. Krüger, M. Müller, C. Drosten and S. Pöhlmann (2020). "The novel coronavirus 2019 (2019-nCoV) uses the SARS-coronavirus

receptor ACE2 and the cellular protease TMPRSS2 for entry into target cells." bioRxiv: 2020.2001.2031.929042.

Hu, M. J., Q. Luo, G. Alitongbieke, S. Y. Chong, C. T. Xu, L. Xie, X. H. Chen, D. Zhang, Y. Q. Zhou, Z. K. Wang, X. H. Ye, L. J. Cai, F. Zhang, H. B. Chen, F. Q. Jiang, H. Fang, S. J. Yang, J. Liu, M. T. Diaz-Meco, Y. Su, H. Zhou, J. Moscat, X. Z. Lin and X. K. Zhang (2017). "Celastrol-Induced Nur77 Interaction with TRAF2 Alleviates Inflammation by Promoting Mitochondrial Ubiquitination and Autophagy." Molecular Cell **66**(1): 141-153.

Huang, C., Y. Wang and X. Li (2020). "Clinical features of patients infected with 2019 novel coronavirus in Wuhan, China " Lancet **395**(10223): 496-496.

Huang, L. L., D. J. Sexton, K. Skogerson, M. Devlin, R. Smith, I. Sanyal, T. Parry, R. Kent, J. Enright, Q. L. Wu, G. Conley, D. DeOliveira, L. Morganelli, M. Ducar, C. R. Wescott and R. C. Ladner (2003). "Novel peptide inhibitors of angiotensin-converting enzyme 2." Journal of Biological Chemistry **278**(18): 15532-15540.

Huang, R., E. Mendis and S. K. Kim (2005). "Improvement of ACE inhibitory activity of chitooligosaccharides (COS) by carboxyl modification." Bioorganic & Medicinal Chemistry **13**(11): 3649-3655.

Imai, Y., K. Kuba, S. Rao, Y. Huan, F. Guo, B. Guan, P. Yang, R. Sarao, T. Wada, H. Leong-Poi, M. A. Crackower, A. Fukamizu, C. C. Hui, L. Hein, S. Uhlig, A. S. Slutsky, C. Y. Jiang and J. M. Penninger (2005). "Angiotensin-converting enzyme 2 protects from severe acute lung failure." Nature **436**(7047): 112-116.

Jiang, F., J. M. Yang, Y. T. Zhang, M. Dong, S. X. Wang, Q. Zhang, F. F. Liu, K. Zhang and C. Zhang (2014). "Angiotensin-converting enzyme 2 and angiotensin 1-7: novel therapeutic targets." Nature Reviews Cardiology **11**(7): 413-426.

Jo, S. H., K. S. Ha, K. S. Moon, J. G. Kim, C. G. Oh, Y. C. Kim, E. Apostolidis and Y. I. Kwon (2013). "Molecular Weight Dependent Glucose Lowering Effect of Low Molecular Weight Chitosan Oligosaccharide (GO2KA1) on Postprandial Blood Glucose Level in SD Rats Model." International Journal of Molecular Sciences **14**(7): 14214-14224.

Kean, T. and M. Thanou (2010). "Biodegradation, biodistribution and toxicity of

chitosan." Advanced Drug Delivery Reviews **62**(1): 3-11.

Kuba, K., Y. Imai, T. Ohto-Nakanishi and J. M. Penninger (2010). "Trilogy of ACE2: A peptidase in the renin-angiotensin system, a SARS receptor, and a partner for amino acid transporters." Pharmacology & Therapeutics **128**(1): 119-128.

Kuba, K., Y. Imai, S. A. Rao, H. Gao, F. Guo, B. Guan, Y. Huan, P. Yang, Y. L. Zhang, W. Deng, L. L. Bao, B. L. Zhang, G. Liu, Z. Wang, M. Chappell, Y. X. Liu, D. X. Zheng, A. Leibbrandt, T. Wada, A. S. Slutsky, D. P. Liu, C. A. Qin, C. Y. Jiang and J. M. Penninger (2005). "A crucial role of angiotensin converting enzyme 2 (ACE2) in SARS coronavirus-induced lung injury." Nature Medicine **11**(8): 875-879.

Liu, Y. X., Y. Yang, C. Zhang, F. M. Huang, F. X. Wang, J. Yuan, Z. Q. Wang, J. X. Li, J. M. Li, C. Feng, Z. Zhang, L. F. Wang, L. Peng, L. Chen, Y. H. Qin, D. D. Zhao, S. G. Tan, L. Yin, J. Xu, C. Z. Zhou, C. Y. Jiang and L. Liu (2020). "Clinical and biochemical indexes from 2019-nCoV infected patients linked to viral loads and lung injury." Science China-Life Sciences **63**(3): 364-374.

Meyer, K. H. and H. Mark (1928). "Concerning the build up of chitin." Berichte Der Deutschen Chemischen Gesellschaft **61**: 1936-1939.

Meyer, K. H. and G. W. Pankow (1935). "On the constitution and structure of chitins." Helvetica Chimica Acta **18**: 589-598.

Nesterenko, M. V., M. Tilley and S. J. Upton (1994). "A simple modification of Blum's silver stain method allows for 30 minute detection of proteins in polyacrylamide gels." Journal of Biochemical and Biophysical Methods **28**(3): 239-242.

Oudit, G. Y., Z. Kassiri, C. Jiang, P. P. Liu, S. M. Poutanen, J. M. Penninger and J. Butany (2009). "SARS-coronavirus modulation of myocardial ACE2 expression and inflammation in patients with SARS." European Journal of Clinical Investigation **39**(7): 618-625.

Patel, V. B., N. Clarke, Z. C. Wang, D. Fan, N. Parajuli, R. Basu, B. Putko, Z. Kassiri, A. J. Turner and G. Y. Oudit (2014). "Angiotensin II induced proteolytic cleavage of myocardial ACE2 is mediated by TACE/ADAM-17: A positive feedback mechanism in the RAS." Journal of Molecular and Cellular Cardiology **66**: 167-176.

Rudall, K. M. (1963). "The Chitin/Protein Complexes of Insect Cuticles." Advances in

Insect Physiology **1**: 257-313.

Sungnak, W., N. Huang, C. Becavin, M. Berg, R. Queen, M. Litvinukova, C. Talavera-Lopez, H. Maatz, D. Reichart, F. Sampaziotis, K. B. Worlock, M. Yoshida, J. L. Barnes and H. L. Biological (2020). "SARS-CoV-2 entry factors are highly expressed in nasal epithelial cells together with innate immune genes." Nature Medicine.

Terrazas, C., S. Oghumu, S. Varikuti, D. Martinez-Saucedo, S. M. Beverley and A. R. Satoskar (2015). "Uncovering Leishmania-macrophage interplay using imaging flow cytometry." Journal of Immunological Methods **423**: 93-98.

Towler, P., B. Staker, S. G. Prasad, S. Menon, J. Tang, T. Parsons, D. Ryan, M. Fisher, D. Williams, N. A. Dales, M. A. Patane and M. W. Pantoliano (2004). "ACE2 X-ray structures reveal a large hinge-bending motion important for inhibitor binding and catalysis." Journal of Biological Chemistry **279**(17): 17996-18007.

Wrapp, D., N. S. Wang, K. S. Corbett, J. A. Goldsmith, C. L. Hsieh, O. Abiona, B. S. Graham and J. S. McLellan (2020). "Cryo-EM structure of the 2019-nCoV spike in the prefusion conformation." Science **367**(6483): 1260-+.

Wu, F., S. Zhao, B. Yu, Y. M. Chen, W. Wang, Z. G. Song, Y. Hu, Z. W. Tao, J. H. Tian, Y. Y. Pei, M. L. Yuan, Y. L. Zhang, F. H. Dai, Y. Liu, Q. M. Wang, J. J. Zheng, L. Xu, E. C. Holmes and Y. Z. Zhang (2020). "A new coronavirus associated with human respiratory disease in China." Nature **579**(7798): 265-+.

Xu, X. T., P. Chen, J. F. Wang, J. N. Feng, H. Zhou, X. Li, W. Zhong and P. Hao (2020). "Evolution of the novel coronavirus from the ongoing Wuhan outbreak and modeling of its spike protein for risk of human transmission." Science China-Life Sciences **63**(3): 457-460.

Yan, R. H., Y. Y. Zhang, Y. N. Li, L. Xia, Y. Y. Guo and Q. Zhou (2020). "Structural basis for the recognition of SARS-CoV-2 by full-length human ACE2." Science **367**(6485): 1444-+.

Yang, X. H., W. Deng, Z. Tong, Y. X. Liu, L. F. Zhang, H. Zhu, H. Gao, L. Huang, Y. L. Liu, C. M. Ma, Y. F. Xu, M. X. Ding, H. K. Deng and C. Qin (2007). "Mice transgenic for human angiotensin-converting enzyme 2 provide a model for SARS coronavirus infection." Comparative Medicine **57**(5): 450-459.

Zhang, H., Z. Kang, H. Gong, D. Xu, J. Wang, Z. Li, X. Cui, J. Xiao, T. Meng, W. Zhou, J. Liu and H. Xu (2020). "The digestive system is a potential route of 2019-nCov infection: a bioinformatics analysis based on single-cell transcriptomes." bioRxiv: 2020.2001.2030.927806.

Zheng, M., D. Qu, H. M. Wang, Z. P. Sun, X. Y. Liu, J. J. Chen, C. G. Li, X. G. Li and Z. Chen (2016). "Intranasal Administration of Chitosan Against Influenza A (H7N9) Virus Infection in a Mouse Model." Scientific Reports **6**.

Zhou, T., B. Zhou and S. L. Huang (2004). "Biocompatible features of chitosan in brain tissues." Chinese Joural of Clinical Rehabilitation(22): 4640-4641.
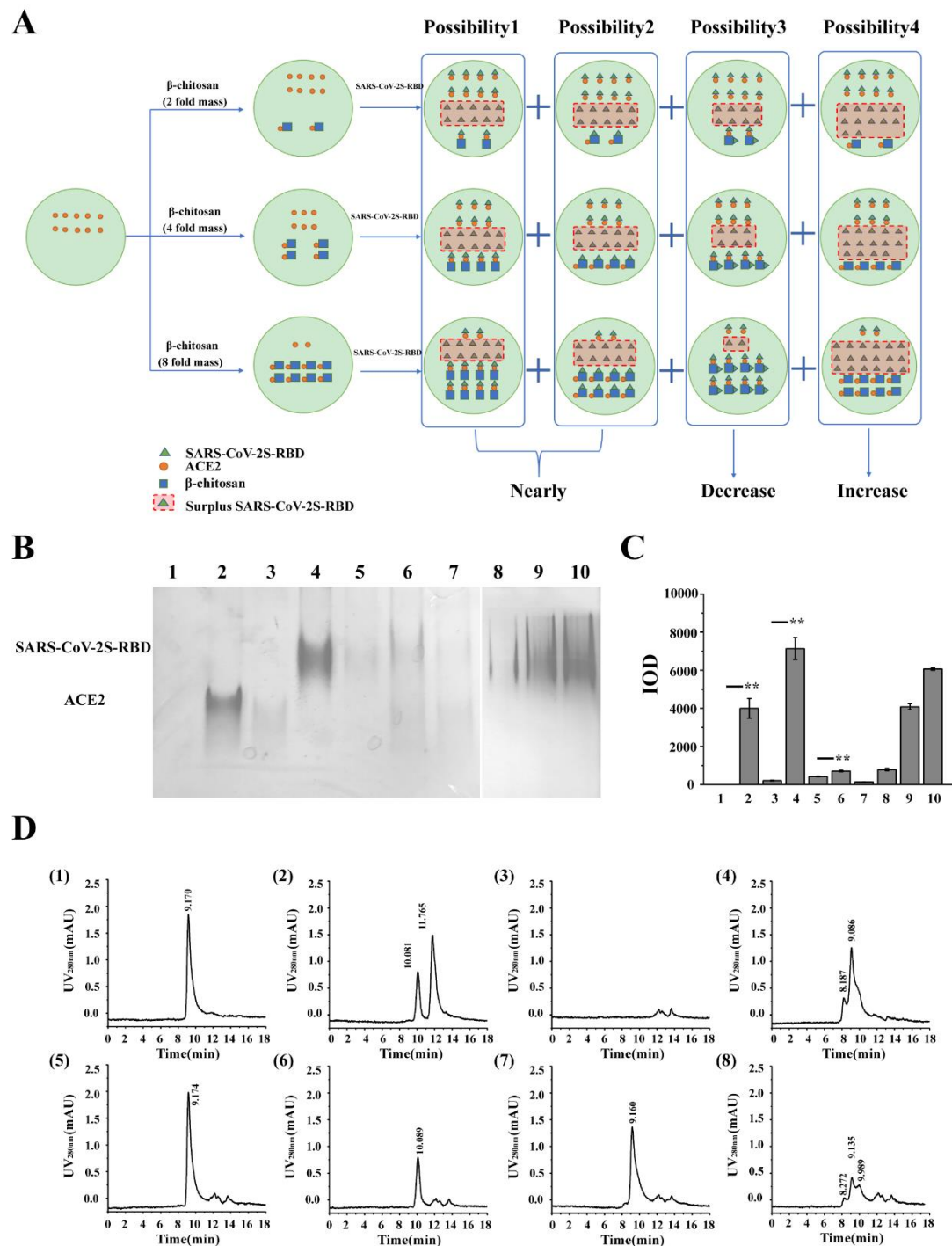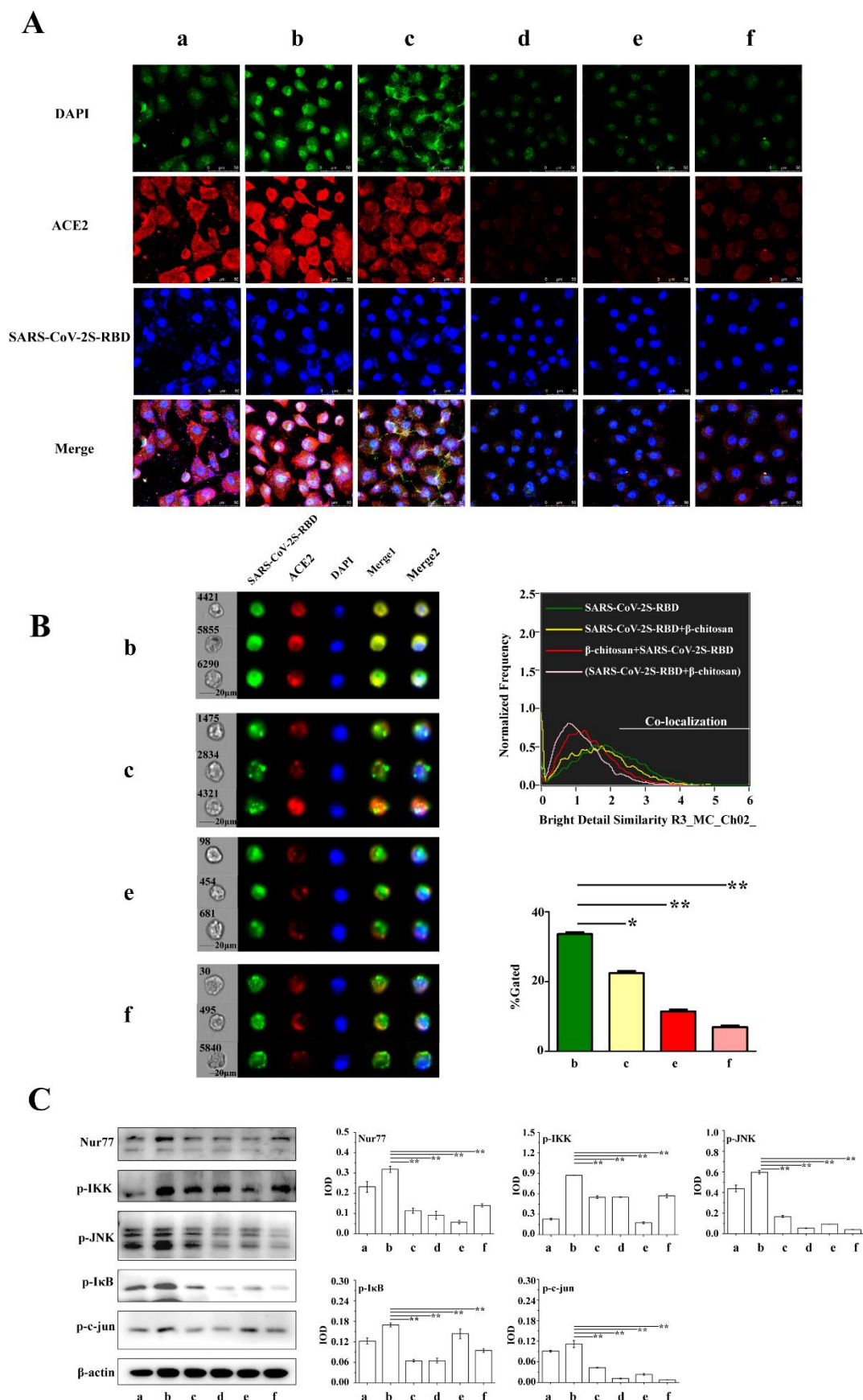
Figure 1. Binding interaction of β-chitosan with SARS-CoV-2-S-RBD/ACE2 by Native-PAGE and HPLC analysis. A: To testify whether the conjugate of β-chitosan and ACE2 can bind with SARS-CoV-2S-RBD again, the experiment was conducted as follows. Under the condition of excessive ACE2 relative to β-chitosan, 1 μg ACE2 were mixed and incubated with 2 μg, 4 μg and 8 μg β-chitosan for 20 min at 37 °C, respectively. Then, 1 μg of SARS-CoV-2-S-RBD were added for co-incubation again in a similar way. Finally, Native-PAGE was used to analyze the binding interaction. B: Native-PAGE analysis of the collected samples. (1).β-chitosan; (2). ACE2; (3). ACE2 + β-chitosan; (4). SARS-CoV-2S-RBD; (5). SARS-CoV-2S-RBD + β-chitosan; (6). ACE2 + SARS-CoV-2S-RBD; (7). (ACE2 + SARS-CoV-2S-RBD) + β-chitosan; (8). (ACE2 + 2 μg β-chitosan) + SARS-CoV-2S-RBD; (9). (ACE2 + 4 μg β-chitosan) + SARS-CoV-2S-RBD; (10). (ACE2 + 8 μg β-chitosan) + SARS-CoV-2S-RBD. C: Integrated option density (IOD) analyzed by Quantity One software. D: HPLC analysis of the collected samples. All the samples were mixed and incubated for 20 mins at 37 °C. (1). ACE2; (2). SARS-CoV-2S-RBD; (3). β-chitosan; (4) ACE2 + SARS-CoV-2S-RBD; (5). ACE2 + β-chitosan; (6). SARS-CoV-2S-RBD + β-chitosan; (7). (ACE2 + SARS-CoV-2S-RBD) + β-chitosan; (8). (ACE2 + β-chitosan) + SARS-CoV-2S-RBD.

Figure 2. Effect of β-chitosan against the binding of SARS-CoV-2S-RBD with ACE2 based

on Vero E6 cell model. A: Effect of β-chitosan against the binding of SARS-CoV-2S-RBD detected by immunofluorescence. B: Effect of β-chitosan against SARS-CoV-2S-RBD binding by flow cytometry. C: Western Blot analysis of inflammation-related proteins. Groups: (a).control; (b). SARS-CoV-2S-RBD; (c). SARS-CoV-2S-RBD + β-chitosan; (d). β-chitosan; (e). β-chitosan + SARS-CoV-2S-RBD; (f). (SARS-CoV-2S-RBD + β-chitosan). **Treatment group (c)**: Cells were treated with SARS-CoV-2S-RBD for 10 min, and then β-chitosan was added for another 10min treatment. **Prevention group (e)**: Cells were treated with β-chitosan for 10 min, and then SARS-CoV-2S-RBD was added for another 10 min treatment. **Group (f)**: β-chitosan and SARS-CoV-2S-RBD were mixed for 10 min in advance, and then the mixture were added to the cells. For other groups, SARS-CoV-2S-RBD or β-chitosan were added into the cells for 10 min, and equal volume of PBS was used as control.
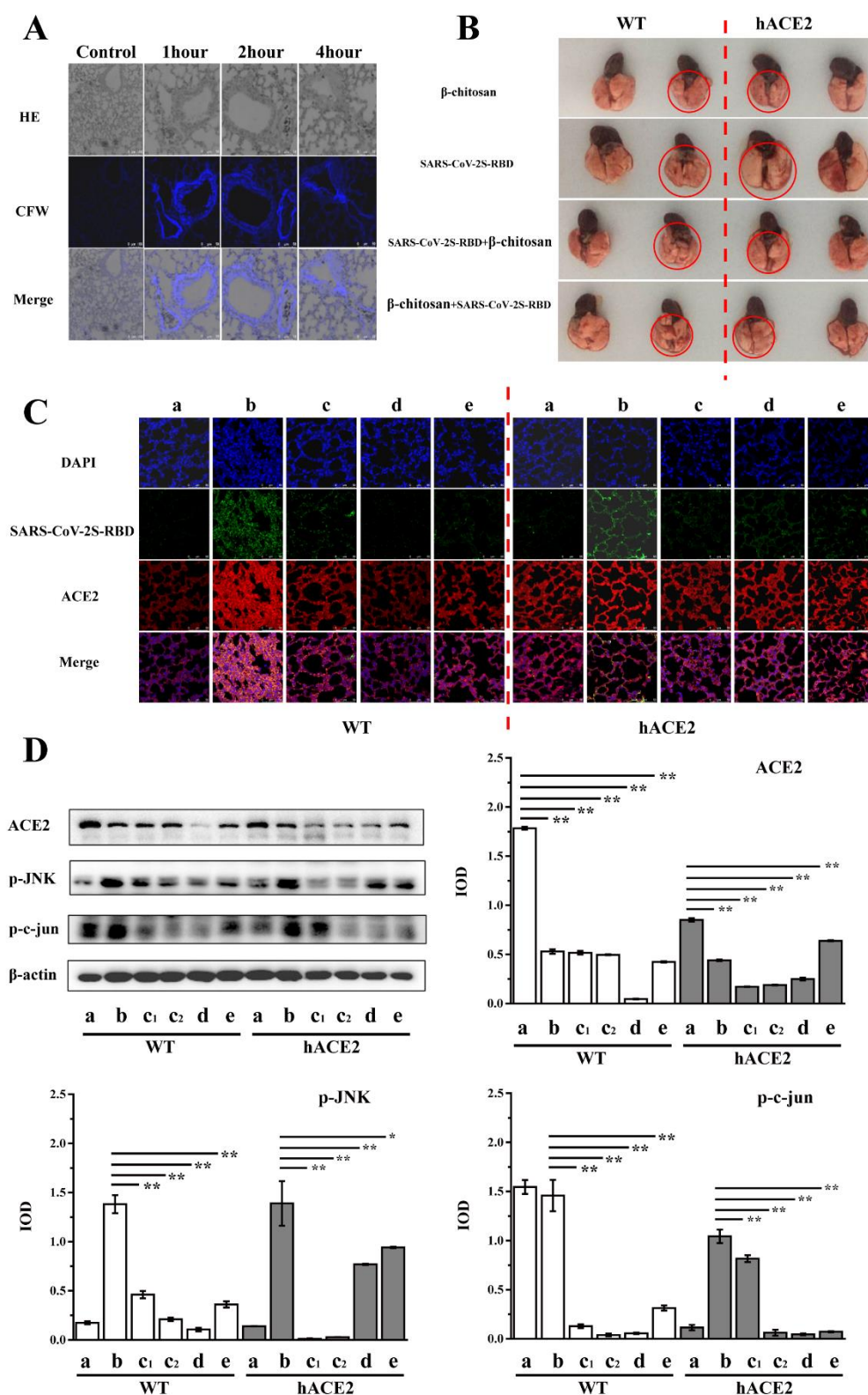
Figure3 Metabolic distribution of β-chitosan and its anti-SARS-CoV-2S-RBD binding in lung tissue of mice. A: Metabolic distribution of FITC labeled β-chitosan in lung tissue in mice; B: Morphological changes of lung organs in mice; C: The expression of ACE2 and its co-localization with SARS-CoV-2S-RBD in WT mice and hACE2 mice observed by immunofluorescence; D: Expression levels of ACE2 and inflammation-related proteins in WT mice and hACE2 mice analyzed by Western Blot.: **Prevention groups (c1 and c2)**: Mice were treated by intranasal administration with 5 mg/kg(L),10 mg/kg(M) β-chitosan

for 1 h, respectively, and then SARS-CoV-2S-RBD was administered for another 1 h treatment. **Treatment group (d)**: Mice were administrated with SARS-CoV-2S-RBD for 1 h, and then 10mg/kg β-chitosan was treated for another 1 h treatment. Groups: (a).control; (b). SARS-CoV-2S-RBD; (c). β-chitosan + SARS-CoV-2S-RBD; (c1). β-chitosan (L) + SARS-CoV-2S-RBD; (c2). β-chitosan (M) + SARS-CoV-2S-RBD; (d). SARS-CoV-2S-RBD + β-chitosan; (e). β-chitosan.
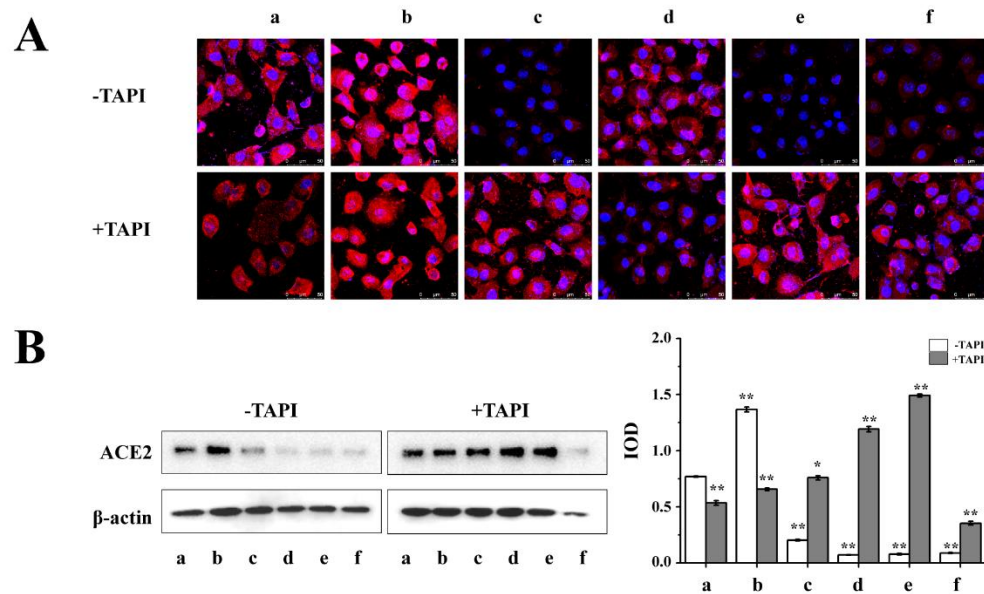
Figure 4 Effect of β-chitosan on ACE2 cleavage activity of ADAM17. A: Effect of ADAM17 inhibitor TAPI on the expression of ACE2 detected by Immunofluorescence. Cells were treated with 8 μM of ADAM17 inhibitor TAPI in advance 30 min. PBS was used as control. For group (b) and (d), cells were treated with SARS-CoV-2S-RBD andβ-chitosan for 10 min, respectively. For group (c), cells were treated with SARS-CoV-2S-RBD for 10 min, and then β-chitosan was added for another 10min treatment. For group (e), cells were treated with β-chitosan for 10 min, and then SARS-CoV-2S-RBD was added for another 10 min treatment. For group (f), β-chitosan and SARS-CoV-2S-RBD were mixed for 10 min in advance, and then the mixture were used to the cells. B: Expression levels of ACE2 and inflammation-related proteins analyzed by Western Blot. Groups: (a).control; (b). SARS-CoV-2S-RBD; (c). SARS-CoV-2S-RBD + β-chitosan; (d). β-chitosan; (e). β-chitosan + SARS-CoV-2S-RBD; (f). (SARS-CoV-2S-RBD + β-chitosan).
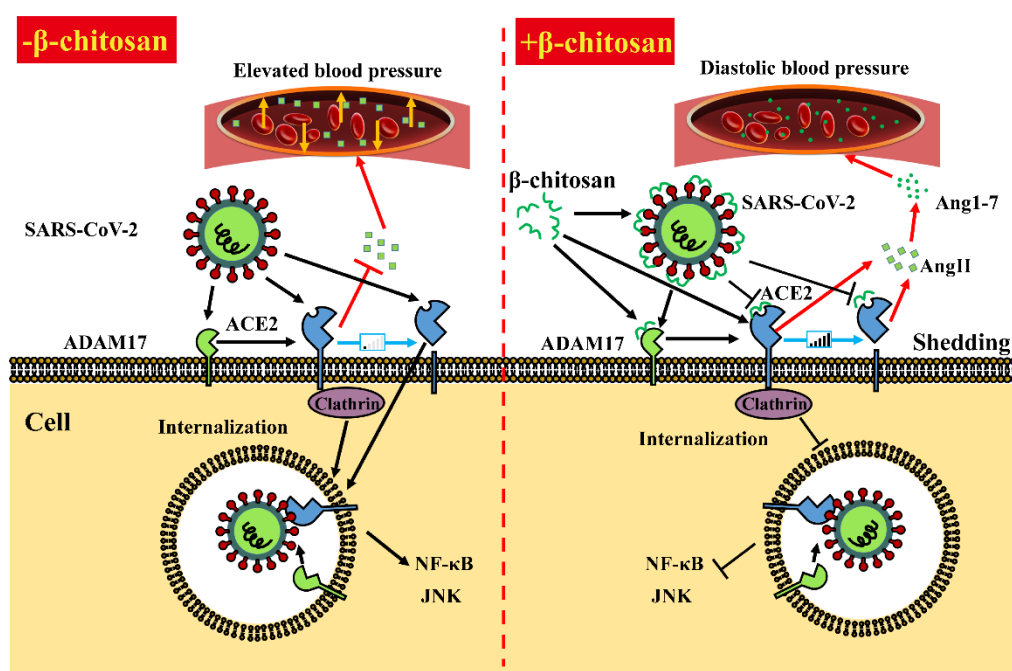
Figure 5 Mechanism of β-chitosan against SARS-CoV-2S-RBD/hACE2 binding